Journal of Photochemistry and Photobiology A: Chemistry 200 (2008) 74–82

Contents lists available at ScienceDirect

Journal of Photochemistry and Photobiology A: Chemistry

journal homepage: www.elsevier.com/locate/jphotochem

High-contrast fluorescence switching using a photoresponsive dithienylethene coordination compound

Hongchun Zhao[a], Usama Al-Atar[a], Tamara C.S. Pace[b], Cornelia Bohne[b], Neil R. Branda[a,*]

[a] 4D LABS, Department of Chemistry, Simon Fraser University, 8888 University Drive, Burnaby, B.C., Canada V5A 1S6
[b] Department of Chemistry, University of Victoria, PO Box 3065, Victoria, B.C., Canada V8W 3V6

ARTICLE INFO

Article history:
Available online 21 June 2008

Keywords:
Photochromism
Molecular switches
Fluorescence

ABSTRACT

A novel hybrid system (**Zn4**) containing a zinc bis(acylamidine) fluorescent dye covalently decorated with two photochromic dithienylethene (DTE) structures was prepared using a concise synthetic route. The photoregulated quenching of the fluorescence from the metal complex was achieved by reversibly switching the DTE component between its two isomers using UV and visible light. The fluorescence quenching can be attributed to intramolecular energy transfer, electron transfer or a combination of the two. Either process is only possible when the DTE is in its ring-closed form (**Zn4b**). The ring-open counterpart (**Zn4a**) lacks an absorption band in the visible region of the spectrum to accommodate energy transfer from the metallobis(acylamidine) to the photochromic DTE, and has an oxidation potential that is too large to match the reduction potential of the metal complex making electron transfer thermodynamically unfavourable. UV–vis absorption and emission spectroscopy demonstrated that the photoregulation of fluorescence has little effect on the photochromic process and the fluorescence could be turned “on” and “off” several times without the appearance of notable side products. The high contrast ratio (~100:1) between the bright and dark states combined with the excellent thermal bistability make the hybrid an excellent candidate for potential use in non-destructive read-out and biological labeling applications, although several limitations need to be overcome (speed of photoswitching, and stability and solubility in water).

1. Introduction

Regulating fluorescence intensity is one of the most attractive uses for molecular photoswitches because of the high sensitivity, resolution, contrast and the fast response times provided by fluorescence technology. Introducing control mechanisms into fluorescence systems would, therefore, offer a convenient means to modulate this versatile optical property. The reversible cyclization reaction of the dithienylethene (DTE) architecture (Scheme 1) has attracted special attention from both fundamental and practical points of view owing to many beneficial properties [1,2]. UV and visible light can be used to toggle the basic structure back and forth (often with a high level of fatigue resistance) between two isomers, each having unique optical and electronic properties. The molecular backbone can be decorated with a wide range of modifying groups to fine-tune the optoelectronic properties of both isomers. This last feature is critical for effective regulation of fluorescence as should be obvious after reading this report.

One application in which it would be useful to photoregulate fluorescence with DTEs is non-destructive data storage where the bright and dark states can be used to code binary information [3–8]. A fluorescent read-out signal offers high sensitivity (often down to the single molecule) and because excitation requires a small number of photons, few side effects are induced to spoil the digitalized signals [9,10].

Biological fluorescence labeling is another setting where regulating fluorescence can be potentially useful. Tracking of particular cell components and events will be facilitated by turning the fluorescent probe “on” and “off” on command [11]. For this application, reversibility and high contrast are critical aspects that must be satisfied. In a related application, better resolution in far-field confocal microscopy can be achieved with spatial resolution below the diffraction limit when photoresponsive DTE derivatives are used [12].

Typically, compounds based on the dithienylethene architecture tend to show very weak fluorescence and are not practical for applications that rely on modulating this optical property. The lack of intense fluorescence has been ascribed to the free rotation around the C–C bonds joining the two thiophene heterocycles to the central cyclopentene ring, which increase the rate of radiationless decay of the excited state [13–16]. Decorating

---

* Corresponding author.
E-mail address: nbranda@sfu.ca (N.R. Branda).

1010-6030/$ – see front matter © 2008 Elsevier B.V. All rights reserved.
doi:10.1016/j.jphotochem.2008.06.010

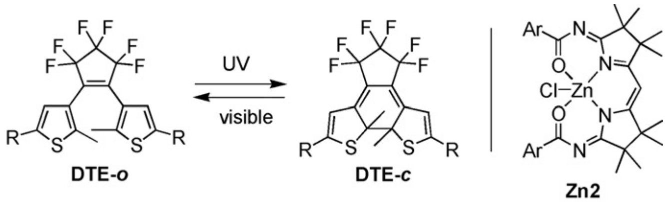

Scheme 1. The reversible cyclization reaction of the dithienylethene architecture between its ring-open (**DTE-*o***) and ring-closed (**DTE-*c***) isomers using UV and visible light, and the highly fluorescent generalized zinc bis(acylamidine) structure **Zn2** used as the fluorescent dye in these studies.

the DTE backbone with a strongly fluorescent molecule overcomes this problem and has been the focus of several studies in which the intensity of emitted light is regulated by converting the DTE between its two isomers. Examples include molecular dyads (DTE–anthracene [17], DTE-diphenylbenzene [18], DTE–oligothiophene [19]), triads (DTE–anthracene–DTE, [20] oligothiophene–DTE–oligothiophene [7,21], porphyrin–DTE–porphyrin [3,4], and BODIPY–DTE–BODIPY [22]) and systems that combine several DTE components with a porphyrin macrocycle [23]. Although significant work has been done to improve the fluorescence quenching efficiency, many examples are restricted by the low fluorescence contrast ratios between the bright and dark states. This report describes the synthesis of a bistable fluorescent photochromic system (**Zn4a**) with a high fluorescence contrast ratio by covalently joining a highly fluorescent zinc bis(acylamidine) dye and two photoresponsive DTE compounds. The two components that make up the hybrid structure were chosen based on their complementary optical properties. As will be clearly demonstrated, the absorbance of only one isomer of the DTE backbone overlaps with the emission band of the metallobis(acylamidine) allowing effective energy transfer from the excited state of the dye to the photochromic component. This is a situation necessary for regulating the emission by toggling the DTE between a quenching and non-quenching isomer. Although the system was designed to harness energy transfer as the quenching mechanism, the possibility of electron transfer should not be excluded as will be discussed in this report. Another critical feature for an effective system is a clear separation of the absorption bands of the two DTE isomers and the fluorescence dye so that each component can be excited without affecting the others. This is also satisfied with hybrid compound **Zn4**.

2. Results and discussion

2.1. Synthesis of bis(DTE), bis(phenyl) and bis(thienyl) coordination compounds *Zn4a*, *Zn5* and *Zn6*

Scheme 2 shows how all the compounds described in this paper are prepared. In all cases, the key component is the bis(amidine) **1**, [24] which can be coupled to aromatic carboxylic acid chlorides to afford the generalized bis(acylated) structure **2**. Metal insertion to produce the neutral zinc complex **Zn2** is achieved by treating ligand **2** with $ZnCl_2$ in the presence of base [25]. These two synthetic steps are used to prepare the photoresponsive coordination compound **Zn4a** (from the acid chloride of DTE **3**), [26] as well as the non-photoactive compounds **Zn5** (from benzoyl chloride) and **Zn6** (from the acid chloride of 5-methyl-thiophene-2-carboxylic acid), which are used for comparative purposes. The preferred method to purify coordination compounds **Zn4a**, **Zn5** and **Zn6** is by recrystallization. Column chromatography is not appropriate because the imines are easily hydrolysed during purification. All new compounds have been characterized by means of ^{1}H and ^{13}C NMR, FT-IR, UV–vis spectroscopy, mass spectrometry and elemental analysis, and the results are consistent with the structures illustrated in Scheme 2.

Care must be taken when treating the metallobis(acylamidine) in subsequent studies. Although they all show high stability when dissolved in CH_2Cl_2, they do not exhibit equivalent stability in other solvents such as CH_3CN and EtOH even when stored in the dark. New bands are observed in both the UV–vis absorption and ^{1}H NMR spectra, [27] changes that are not observed for equivalent CH_2Cl_2 solutions of **Zn4a** or **Zn5** or for the equivalent free-base ligands. The structures produced in these solutions have yet to be isolated and characterized.

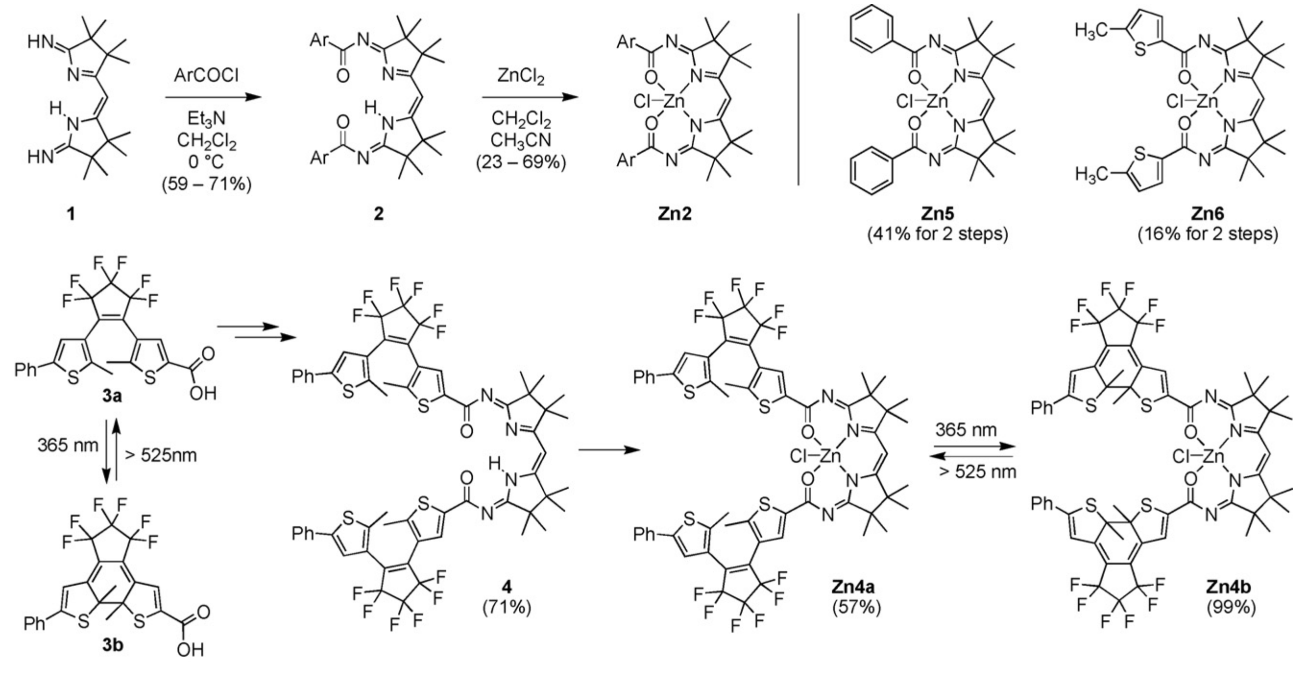

Scheme 2. Synthesis and photoreactions of the compounds reported in this paper.

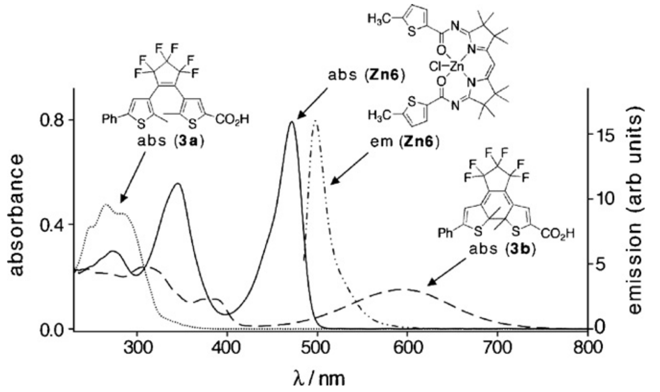

Fig. 1. UV–vis absorption spectra of CH_2Cl_2 solutions of DTE **3** (2×10^{-5} M) in its ring-open (···) and ring-closed (- - -) forms, the bis(thienyl) coordination compound **Zn6** (1.3×10^{-5} M) (-), and the emission spectrum of a CH_2Cl_2 solution of **Zn6** (– · · –) using 475 nm as the excitation wavelength.

2.2. UV–vis absorption and emission spectroscopy

Fig. 1 illustrates why the two particular molecular components (the DTE decorated with a phenyl ring on one side and a carbonyl group on the other (e.g. **3**), and zinc complex **Zn2**) are well suited for use in photomodulating fluorescence. As mentioned in the introduction to this paper, it is critical that the absorption bands of both isomers of the photoswitch do not overlap with the absorption band of the fluorophore, while the band for only one of the isomers should overlap as much as possible with the dye's emission band. This is the case for the components used to build structure **Zn4** as demonstrated by comparing the absorption and emission spectra of model compound **Zn6** and carboxylic acid **3**, which are good representations of the two components.

The UV–vis absorption spectrum of model complex **Zn6** shows that it has an intense absorption band at 472 nm (Fig. 1 and Table 1), which is not present in the free ligand **6** [28] revealing the importance of the metal in this project. This band appears in between those for the ring-open and ring-closed isomers of the carboxylic acid (284 nm for **3a**; 597 and 383 nm for **3b**) [29] and can be used to specifically generate the excited state of the coordination complex without exciting either isomer of the photoresponsive DTE component. Fig. 1 also shows the emission spectrum of compound **Zn6**. Irradiating a CH_2Cl_2 solution of **Zn6** with 475 nm light produces an intense and narrow emission band centred at 498 nm. While there is no overlap between this emission band and the absorption band of the ring-open isomer (**3a**), there is significant overlap with the absorption band of the ring-closed equivalent (**3b**), a necessary condition for selectively quenching the emission of the Zn-coordination component through energy transfer by only one DTE photoisomer.

Table 1
Selected absorption and emission data for compounds **3a**, **3b**, **Zn6**, **4a**, **4b**, **Zn4a** and **Zn4b**[a]

Compound	Absorbance (nm)	$\lambda_{emission}$ (nm)
3a	248/267/284	–
3b	309/383/597	–
Zn6	345/472	498[c]
4a	281/376	–
4b	267/307[b]/392/611	–
Zn4a	281/342/478	502[d]
Zn4b	279/340[b]/479/665	–

[a] All spectra were measured using CH_2Cl_2 solutions ranging from 1 to 2×10^{-5} M.
[b] Appears as a shoulder.
[c] λ_{ex} = 475 nm.
[d] λ_{ex} = 470 nm.

2.3. Photoregulation of UV–vis absorption and emission properties

The photoinduced conversion of the ring-open isomer of the hybrid compound (**Zn4a**) to its ring-closed counterpart (**Zn4a**) is easily monitored using UV–vis spectroscopy as illustrated in Fig. 2a. Irradiating a CH_2Cl_2 solution of the complex with UV light (365 nm) [29] results in a decrease in the high-energy absorption bands corresponding to the ring-open isomer and an accompanying appearance of a broad absorption band in the visible spectral region that corresponds to ring-closed isomer (λ_{max} = 665 nm, Table 1). These spectral changes are responsible for the change in colour of the solution from yellow to blue–green as the photostationary state is reached. ^1H NMR spectroscopy reveals that the photostationary state contains almost quantitative amounts (at least 99%) of the ring-closed isomer (Fig. 2b and c) [30]. The pattern of peaks in the ^1H NMR spectrum also clearly reveals that only one of the photochromic DTE units in **Zn4a** is undergoing photocyclization, a phenomenon that has been observed for multi-component DTE derivatives in the past [23,31]. In the case of compound **Zn4a**, the product of the photoreaction is **Zn4c** and not the structure shown in Scheme 2.

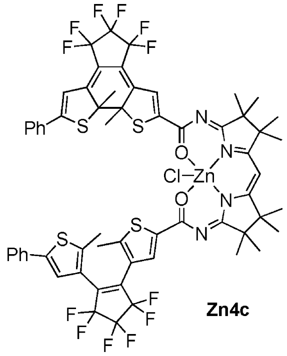

Zn4c

Irradiation of the coloured solution containing the ring-closed isomer (**Zn4c**) with visible light at wavelengths of 525 nm [32] and greater regenerates the original spectrum corresponding to the ring-open isomer and the colour of the solution changes back to yellow. These ring-closing/ring-opening cycles can be repeated (at least 10 times) without any observable variation in the UV–vis spectrum of either isomer (inset in Fig. 2a). Also, extended periods of continuous irradiation (as much as 2 h) of these solutions with 365 nm light do not result in any observable decomposition of the compound as attested by ^1H NMR spectroscopy although the UV–vis shows a small amount of spectral variation. The ring-closed isomer (**Zn4c**) in the photostationary state is also stable in CD_2Cl_2 solutions for at least 2 weeks in the dark.

Metal insertion has an advantageous effect on the optical properties of the photoresponsive compound described in this paper. The presence of zinc not only produces a new absorbance (centred at 478 nm in the case of **Zn4**) as was reported for bis(thiophene) compound **Zn6**, it also increases the optical region in which the DTE components are transparent by inducing a 50 nm bathochromic shift of the lowest-energy absorbance for the ring-closed isomer from 611 nm (without Zn, **4c**) to 665 nm (with Zn, **Zn4c**) while having little effect on properties of the ring-open isomer. The presence of bis(acylamidine)'s Soret band at 478 nm allows this chromophore to be selectively irradiated to induce fluorescence and a CH_2Cl_2 solution of the ring-open isomer of the hybrid compound (**Zn4a**) displays intense fluorescence at 502 nm when excited at 470 nm as shown in Fig. 2f. Converting isomer **Zn4a** into its ring-closed counterpart by irradiating a solution of it with 365 nm light results in a decrease in the fluorescence intensity at 502 nm to one that is at

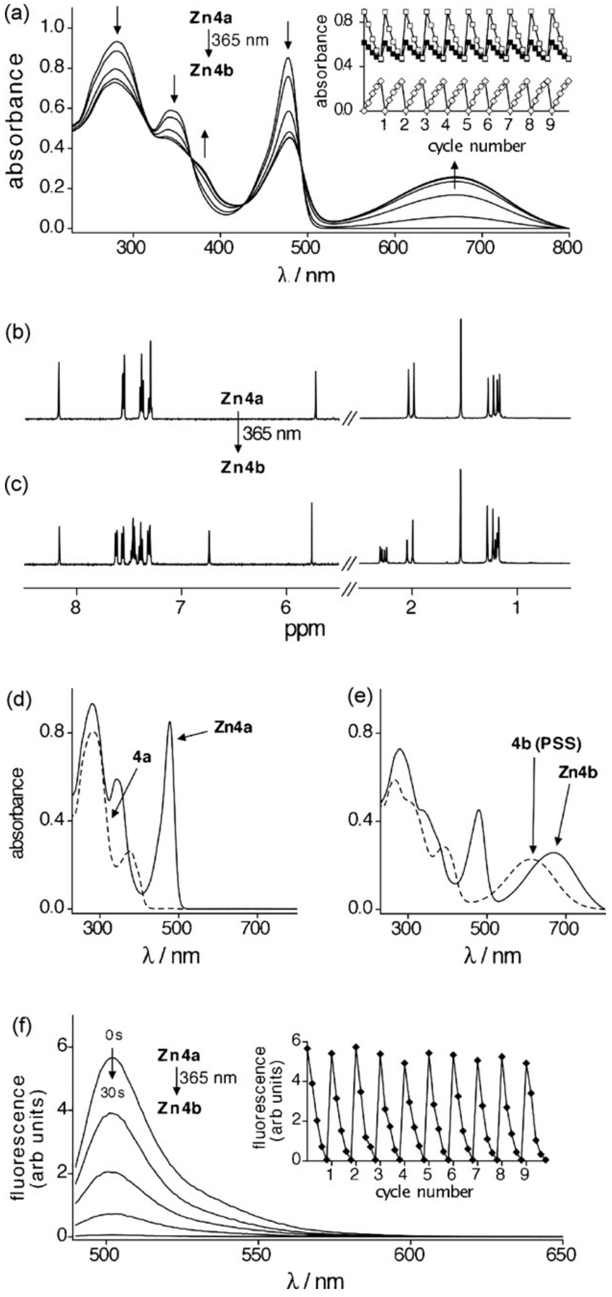

Fig. 2. (a) Changes in the UV–vis spectra of a CH_2Cl_2 solution (1.3×10^{-5} M) of **Zn4a** when irradiated with 365 nm light for 0, 2, 5, 10, 20 and 30 s. The solution was deoxygenated by subjecting it to freeze–pump–thaw cycles. The inset shows modulated absorption at 343 nm (■) and 478 nm (□) corresponding to absorbances for the ring-open isomer (**Zn4a**), and at 665 nm (◊) corresponding to the absorbance for the ring-closed (**Zn4b**) isomer during alternating irradiation at 365 nm (2, 5, 10 and 30 s) and greater than 525 nm (180 s). ^1H NMR spectra of CD_2Cl_2 solutions of complex **Zn4a** (b) before irradiation and (c) after irradiation (365 nm) for 120 min. (d) UV–vis absorption spectra of CH_2Cl_2 solutions of **4a** and **Zn4a**, and (e) the photostationary states obtained when solutions of **4a** and **Zn4a** are irradiated with UV light (365 nm) until no changes in the spectra were observed (120 s for **4a** and 30 s for **Zn4a**). (f) Changes in the emission spectra of a CH_2Cl_2 solution (1.3×10^{-5} M) of **Zn4a** when it is irradiated with 365 nm light for 0, 2, 5, 10, 20 and 30 s (λ_{ex} = 470 nm). The inset shows modulated emission at 502 nm during alternating irradiation at 365 nm (2, 5, 10 and 40 s) and greater than 525 nm (6 min).

the lower limits of the fluorescence detector showing the effective photoregulation of fluorescence by the photochromic component. This quenching is presumably a result of intramolecular energy transfer between the two components in **Zn4c**, although as will be seen later in this report, photoinduced electron transfer cannot be ruled out. In an analogous fashion to what has already been described for the UV–vis absorption properties of the hybrid compound, the original fluorescence can be regenerated when the solution the **Zn4c** is irradiated with light of wavelengths longer than 525 nm. The fluorescence of **Zn4** can be reversibly modulated by cycling the compound between its ring-open and ring-closed isomers by alternating the light used for irradiation between UV and visible as shown in the inset to Fig. 2f. Little degradation in the compound's optical properties is observed during these experiments.

The isolation of the spectral bands is not perfect, however, and irradiation at either the excitation (470 nm) or emission wavelength (502 nm) results in a very small amount (1%) of ring-closing and ring-opening, respectively. Prolonged excitation of the ring-open isomer at 470 nm would, therefore, result in a decrease in the fluorescence intensity as **Zn4a** is converted to its ring-closed counterpart. Despite this minor limitation, the hybrid system is an attractive candidate for potential use in applications where selective fluorescence quenching is required. Our interests are in developing new photochromic compounds with high emission efficiency, signal-to-noise and contrast ratios, and sensitivity to satisfy the requirements for many materials science applications and the **Zn4a** ⇆ **Zn4c** meet these requirements. The fluorescence contrast between bright and dark states at 502 nm is very high (98:1).

2.4. *Fluorescence quantum yields and lifetimes*

The fluorescence quantum yield of **Zn4a** in CH_2Cl_2 is 0.12 ± 0.02, measured as an average of two independent experiments using quinine bisulfate in 0.5 M H_2SO_4 as the primary standard ($\Phi_f = 0.55$) and 320 nm as the excitation wavelength [33]. The quantum yield shows no dependence on concentration, however, some error will have been introduced into this number by the fact that a small amount of switching (**Zn4a** → **Zn4c**) occurs during irradiation in the fluorimeter, with absorbance at 470 nm decreasing by approximately 10%. The measured quantum yield is comparable to fluorescent photochromic systems reported by other authors as 0.12, [34] 0.03 [35] and 0.22 [36].

Fluorescence lifetimes are 1.40 ± 0.05 ns as measured for two different solutions using time-resolved techniques. In one case, only the ring-open isomer (**Zn4a**) is present in solution, since no absorption bands are observed in the visible region of the UV–vis absorption spectrum. For a second solution, a mixture of ring-open and ring-closed isomers is generated by irradiating the sample with UV light (365 nm). In both cases, the fluorescence decay (Fig. 3) is mono-exponential and the same lifetime is measured, which implies the presence of only one fluorescent species (i.e. the ring-open isomer **Zn4a**). The ring-closed form is non-fluorescent (at least within the limits of the equipment used in the experiments). Little change in the absorbance spectra over the course of the experiments is observed, indicating that a minimal amount of switching occurs.

2.5. *Electrochemistry of carboxylic acid **3a** and bis(phenyl) model compound **Zn5***

Although **Zn4a** was designed to take advantage of energy transfer to quench fluorescence, photoinduced electron transfer (PET) should not be ruled out as a possible quenching mechanism. Photoregulating fluorescence by this mechanism relies on a difference in the electron donating ability between the ring-open and ring-closed isomers of the DTE component, which can be assessed using cyclic voltammetry and model compounds **3a** and **3b**. The cyclic voltammograms (CV) measured on CH_2Cl_2 solutions (1.0×10^{-3} M)

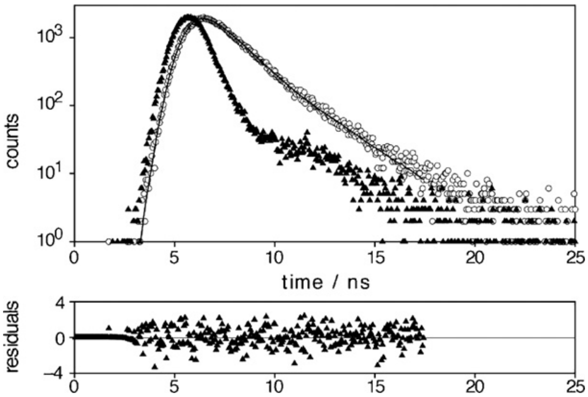

Fig. 3. Time-resolved fluorescence decay of **Zn4a** in CH_2Cl_2 fit to a mono-exponential function (decay (◯), instrument response function (▲), fit (–)). The residuals, indicating the quality of the fit, are shown below the decay. Excitation was carried out at 470 nm with emission at 502 nm.

of both isomers are shown in Fig. 4. Both isomers undergo irreversible oxidations at high potentials (+1.570 V (1.806 versus NHE) for **3a** and +1.224 V (1.460 V versus NHE) for **3b**), however, the ring-closed isomer has an additional oxidation peaks appearing at +0.703 V (0.939 V versus NHE) and a reduction peak at −1.123 V (−0.887 V versus NHE). The CV the bis(phenyl) imidate model compound **Zn5** shows that it undergoes reversible reduction at −1.016 V (−0.945 V versus NHE). These valued can be used to estimate the free energies of photoinduced electron transfer as described below.

2.6. Free energy of PET calculations

The calculated negative value of $-13.36\ \mathrm{kcal\,mol^{-1}}$ for the free energy for PET in **Zn5**·**3b** (see experimental section for details) indicates that the reaction is thermodynamically favourable for the ring-closed isomer of the DTE component when it acts as the electron donor and the **Zn5** acts as the electron acceptor. On the other hand, the free energy for the PET reaction using the ring-open isomer (**3a**) is $+6.73\ \mathrm{kcal\,mol^{-1}}$, which suggests that electron transfer is highly unlikely in **Zn**·**3b**. These estimates support the claim that PET may also be responsible for photoregulating fluorescence quenching in the hybrid system **Zn4**. The exact mechanism for the quenching process has yet to be determined.

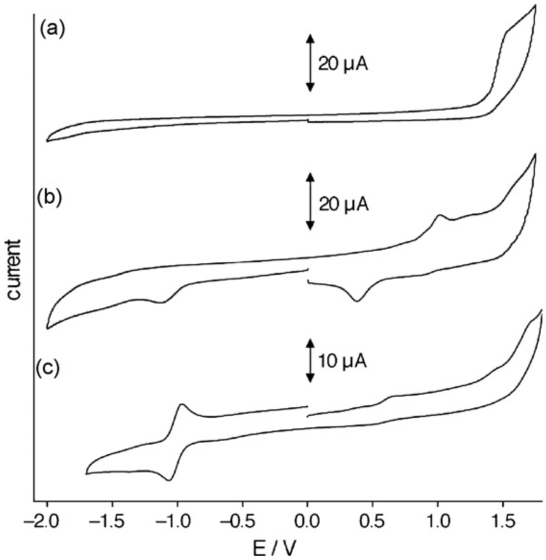

Fig. 4. CVs of CH_2Cl_2 solutions (1.0×10^{-3} M) of (a) ring-open isomer **3a**, (b) ring-closed isomer **3c** and (c) bis(acylamidine) **Zn5**. The photostationary state of **3b** was generated with 365 nm light.

Table 2
Preparation and thickness measurements of films prepared by spin-casting solutions of **Zn4a** and PMMA[a]

Film	**Zn4a** (mg)	PMMA (mg)	Spin rate (rpm)[b]	Film thickness (nm)
1	2.0	16.5	6000	568
2	0.8	8.8	3000	225
3	0.5	5.6	3000	166

[a] All films were prepared using PMMA with an average of molecular weight of 120 000 and 0.2 mL of $CHCl_3$.

[b] For 2 min.

2.7. Photochromism and regulation of fluorescence in thin films

The application of fluorescence photoregulation to technologies such as non-destructive data storage demands the incorporation of the compounds into films that retain the operation of the system in the practical device. With this in mind, the hybrid Zn bis(acylamidine) **Zn4a** can be immobilized in thin films of PMMA by spin-casting $CHCl_3$ solutions of it onto quartz substrates (Table 2). A thicker film (568 nm) is appropriate for absorption spectroscopy where a longer pathlength is required (Fig. 5a), while the emission properties are best characterized using thinner films (150–250 nm) (Fig. 5b).

In an analogous manner to how the solutions of the photochromic compounds were treated, all films of **Zn4a**·PMMA can be irradiated with 365 nm light to trigger the ring-closing reactions and generate coloured films containing the ring-closed isomer (**Zn4c**). Photobleaching is accomplished by using light with wave-

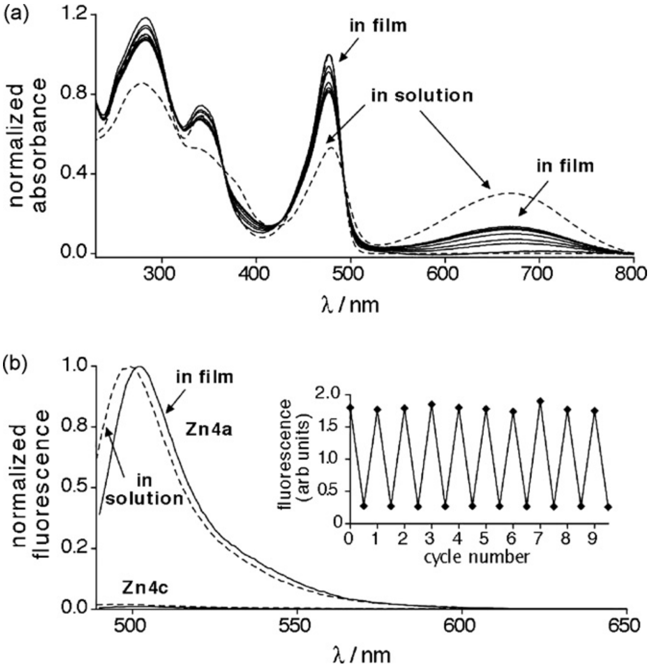

Fig. 5. (a) Changes in the UV–vis spectra of **Zn4a** when cast as a thin film (–) and irradiated with 365 nm light for 0, 5, 15, 60, 120, 180 and 240 s. The spectra have been normalized at 479 nm and those for a CH_2Cl_2 solution of **Zn4a** and **Zn4b** (- - -) have been included for comparison. (b) The emission spectra of **Zn4a** when cast as a thin film before and after irradiating it with 365 nm light for 120 s (–). The inset shows modulated emission ($\lambda_{ex} = 470$ nm) at 499 nm during alternating irradiation at 365 nm (240 s) and greater than 502 nm (5 min). The spectra have been normalized at 499 nm and those for a CH_2Cl_2 solution of **Zn4a** and **Zn4c** (- - -) have been included for comparison.

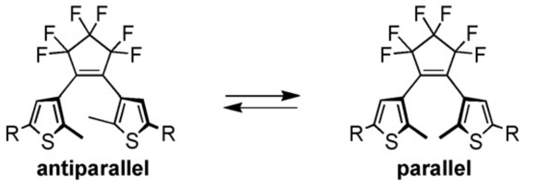

Scheme 3. Spontaneous interconversion of two conformation of the DTE architecture.

lengths longer than 525 nm, which as it does for the solutions, regenerates the ring-open isomer. When excited at 470 nm, the films emit light at 499 nm when the hybrid is in its ring-open form. The emission for the photostationary state in the film decreases almost to the baseline. However, compared to solution, the contrast ratio between the bright and dark states in the film is smaller (49:1) than what it is in solution. The rate of ring-closing is also smaller and the percentage of the ring-closed isomers in the photostationary state is less than what it is for the solutions. The decrease in photoresponse may be due to the fact that the rigid solid-state matrix restricts the conformational flexibility required to convert the unproductive parallel conformation to the productive anti-parallel one (Scheme 3) as has been seen in other systems [37].

3. Conclusions

In this report, we describe a novel hybrid system that combines the advantageous features of a highly fluorescent zinc bis(acylamidine) with the reversible photoresponse of the dithienylethene backbone to regulate emission in solution and the solid-state. Only the ring-open isomer allows the fluorescence at 502 nm. The ring-closed isomer, on the other hand, effectively quenches the emission. The fluorescence switching process can be turned “on” and “off” for ten cycles without formation of notable side products.

To make this system useful in practical applications faster cyclization rates and higher photostationary states would be required in the solid-state. The reduced stability of the metallobis(acylamidine)s in polar solvents also limits their use in the aqueous environment necessary for practical use in biological applications. Not only would future generations of photoresponsive fluorescence quenchers benefit from enhanced stability, they must also offer greater water solubility. The cobalt analogue of hybrid **Zn4a** may represent a more water-soluble version, however, the preparation of this compound following the procedures described by Scheffold [24] has yet to be achieved [38].

4. Experimental

4.1. Materials

All solvents used for synthesis and spectroscopy were dried and degassed by passing them through steel columns containing activated alumina under nitrogen using an MBraun solvent purification system with the exception of the solvents used for NMR analysis (Cambridge Isotope Laboratories), which were used as received. Column chromatography was performed using silica gel 60 (230–400 mesh) from Silicycle Inc. The volumes of all eluant solvents are reported in % v/v. All reagents and starting materials were purchased from Aldrich and used as received with the exception of the bis(amidine) **1**, which was kindly provided by Dr. C. Weymuth (University of Zurich), and the Bu_4NPF_6 electrolyte which was recrystallized three times from EtOH and dried in vacuo at 110 °C for 3 days prior to use.

4.2. General techniques

^{1}H and ^{13}C NMR characterizations were performed on a Bruker AMX 400 instrument working at 400.103 MHz for ^{1}H NMR and 100.610 MHz for ^{13}C NMR spectroscopy or a Varian Inova 500 instrument working at 499.77 MHz for ^{1}H NMR and 125.68 MHz for ^{13}C NMR spectroscopy. Chemical shifts (δ) are reported in parts per million relative to tetramethylsilane using the residual solvent peak as a reference standard. Coupling constants (J) are reported in Hertz. FT-IR measurements were performed using a Nicolet Nexus 670 instrument. Mass spectrometry was performed using a Waters matrix assisted laser desorption /ionization (MALDI) or an HP5985 mass spectrometer with isobutane as the chemical ionization source for low resolution mass spectrometry (LRMS). Elemental analyses were performed using a Kratos Concept-H instrument with perfluorokerosene as the standard. Melting point measurements were performed using a Fisher-Johns Melting Point Apparatus. UV–vis absorption and fluorescence measurements were performed using a Varian Cary 300 Bio spectrophotometer and a PTI QM-2000-4 scanning spectrofluorometer with the slits set to a bandpass of 2 nm, respectively.

*4.3. Synthesis of the diphenyl version of ligand **2** (Ar = C_6H_6)*

A solution of bis(amidine) **1** (300 mg, 1.04 mmol) and Et_3N (0.35 mL, 2.5 mmol) in anhydrous CH_2Cl_2 (25 mL) was treated dropwise over 5 min with a solution of benzoyl chloride (0.27 mL, 2.3 mmol) at 0 °C under an N_2 atmosphere. After 30 min of stirring, the cooling bath was removed and the reaction was allowed to slowly warm to room temperature and stirred there for 2 h. The solvent was evaporated to form a slurry, which was loaded onto a short silica column (25 g silica, 4 cm high, CH_2Cl_2, 2.5% CH_3OH, 1% Et_3N). The yellow solution was collected and evaporated to dryness resulting in a mixture of a yellow solid and a viscous oil. This mixture was washed with Et_2O and the yellow solid was collected by vacuum filtration. Purification by recrystallization (CH_2Cl_2 and Et_2O) afforded 351 mg (59%) of the diphenyl version of ligand **2** as yellow crystals. mp = 202–207 °C. ^{1}H NMR ($CDCl_3$, 500 MHz): δ 12.70 (br s, 1H), 8.20 (d, J = 7.8 Hz, 4H), 7.50 (t, J = 7.8 Hz, 2H), 7.42 (t, J = 7.8 Hz, 4H), 5.32 (s, 1H), 1.22 (s, 12H), 1.16 (s, 12H). ^{13}C NMR ($CDCl_3$, 125 MHz): δ 181.8, 179.1, 175.7, 135.7, 132.3, 130.2, 128.0, 89.6, 49.3, 47.8, 23.6, 22.8. FT-IR (KBr cast): 3433, 3263, 3067, 2973, 1662, 1622, 1658, 1497, 1379, 1317, 1281, 1245, 1142, 1112, 1075, 1058, 1025, 783, 721, 691 cm^{-1}. MALDI m/z = 497 [M + H]$^+$. Anal. Calcd for $C_{61}H_{52}N_4O_2S_4F_{12}$: C, 74.97; H, 7.31; N, 11.28. Found: C, 74.67; H, 7.36; N, 11.56.

*4.4. Synthesis of the diphenyl coordination compound **Zn5***

A solution of the diphenyl version of ligand **2** (Ar = C_6H_6) (100 mg, 0.2 mmol) and Et_3N (56 μL, 0.40 mmol) in anhydrous CH_2Cl_2 (25 mL) was treated with a solution of anhydrous $ZnCl_2$ (137 mg, 1.01 mmol) in anhydrous CH_3CN (25 mL) under an N_2 atmosphere. The resulting solution was stirred for 0.5 h at room temperature at which time it was evaporated to a slurry. The slurry was loaded onto a short silica column (15 g silica, 2 cm high, CH_2Cl_2, 5% CH_3OH). The yellow solution was collected and evaporated to dryness. The resulted solid yellow residue was redissolved in CH_2Cl_2 and any insoluble solids were filtered off. The filtrate was washed with water (5 mL) and the organic layer was separated and evaporated in vacuo. Purification by recrystallization (two times), first using CH_2Cl_2 and Et_2O and then using $CHCl_3$ and Et_2O yielded 83 mg (69%) of **Zn5** as bright yellow cottony crystals. mp = 265–270 °C. ^{1}H NMR ($CDCl_3$, 500 MHz): δ 8.55 (d, J = 7.8 Hz, 4H), 7.59 (t, J = 7.8 Hz, 2H), 7.49 (t, J = 7.8 Hz, 4H), 5.67

(s, 1H), 1.32–1.17 (m, 24H). ^{13}C NMR ($CDCl_3$, 100 MHz): δ 196.1, 196.0, 180.8, 136.7, 133.7, 131.5, 128.3, 93.2, 51.2, 50.5, 25.3, 23.9, 23.2, 22.6 (14 of 21 carbons found). FT-IR (KBr cast): 3449, 2976, 1619, 1554, 1493, 1384, 1317, 1261, 1133, 1109, 1089, 1075, 1059, 1023, 778, 695 cm^{-1}. MALDI m/z = 596 [M + H]$^+$. Anal. Calcd for $C_{61}H_{52}N_4O_2S_4F_{12}$: C, 62.42; H, 5.91; N, 9.39. Found: C, 62.68; H, 5.98; N, 9.60.

*4.5. Synthesis of the bis(5-methylthienyl) version of ligand **2** (Ar = thiophene)*

A solution of bis(amidine) **1** (341 mg, 1.18 mmol) and Et_3N (0.36 mL, 2.6 mmol) in anhydrous CH_2Cl_2 (25 mL) was treated with 5-methyl-2-thiophenecarboxylic acid chloride [26] (0.42 g, 2.60 mmol) at 0 °C under an N_2 atmosphere. After stirring for 30 min, the cooling bath was removed and the reaction was allowed to slowly warm to room temperature and stirred there for 2 h. The solution was evaporated to a slurry, which was loaded onto a short silica column (27 g silica, 4 cm high, CH_2Cl_2, 2.5% CH_3OH, 1% Et_3N). The yellow solution was collected and evaporated to dryness resulting in a mixture of a yellow solid and a viscous oil. The mixture was washed with Et_2O and the yellow solid was collected by filtration. Purification by recrystallization (CH_3OH) yielded 445 mg (70%) of the thiophene version of ligand **2** as brown crystals. mp = 202–203 °C. ^{1}H NMR ($CDCl_3$, 400 MHz): δ 12.73 (br s, 1H) 7.73 (d, J = 3.9 Hz, 2H), 6.77 (d, J = 3.9 Hz, 2H), 5.30 (s, 1H), 2.52 (s, 6H), 1.18 (s, 12H), 1.14 (s, 12H). ^{13}C NMR ($CDCl_3$, 100 MHz): δ 181.8, 175.9, 173.3, 147.9, 138.7, 133.6, 126.5, 89.5, 49.3, 47.7, 23.5,22.7, 16.1. FT-IR (KBr cast) 3435, 3210, 2971, 1686, 1644, 1611, 1589, 1494, 1456, 1281, 1249, 1141, 1058, 828, 796 cm^{-1}. MALDI m/z = 536 [M + H]$^+$. Anal. Calcd for $C_{29}H_{36}N_4O_2S_2$: C, 64.89; H, 6.76; N, 10.44. Found: C, 65.21; H, 6.56; N, 10.72.

*4.6. Synthesis of the bis(5-methylthienyl) coordination compound **Zn6***

A solution of the bis(5-methylthienyl) version of ligand **2** (100 mg, 0.19 mmol) and Et_3N (52 μL) in anhydrous CH_2Cl_2 (25 mL) was treated with a solution of the anhydrous $ZnCl_2$ (127 mg, 0.93 mmol) in anhydrous CH_3CN (25 mL) under an N_2 atmosphere. The solution was stirred for 2 h and evaporated to a slurry. The slurry was loaded onto a short silica column (20 g silica, 3 cm high, CH_2Cl_2, 5% CH_3OH). The yellow solution was collected and evaporated to dryness. The resulted yellow solid was redissolved in CH_2Cl_2 and any insoluble solids were filtered off. The filtrate was washed with water (5 mL) and the organic layer was separated and evaporated in vacuo. Purification by recrystallization (CH_3CN and Et_2O) yielded 27 mg (23%) of **Zn6** as bright orange crystals. mp = 247–248 °C. ^{1}H NMR ($CDCl_3$, 500 MHz): δ 8.00 (d, J = 3.9 Hz, 2H), 6.84 (d, J = 3.9 Hz, 2H), 5.58 (s, 1H), 2.55 (s, 6H), 1.32–1.12 (m, 24H). ^{13}C NMR ($CDCl_3$, 100 MHz): δ 195.3, 190.0, 175.0, 151.5, 140.3, 136.2, 127.5, 92.7, 50.7, 50.4, 24.5, 24.4, 23.0, 21.9, 16.3 (15 of 22 carbons found). FT-IR (KBr cast): 3435, 3210, 2971, 1686, 1644, 1611, 1589, 1494, 1456, 1281, 1249, 1141, 1058, 828, 796 cm^{-1}. MALDI m/z = 634 [M + H]$^+$.

*4.7. Synthesis of the carboxylic acid chloride of DTE **3***

A solution of carboxylic acid **3** (0.29 g, 0.59 mmol) and anhydrous DMF (33 μL) in anhydrous CH_2Cl_2 (50 mL) was cooled to 0 °C and treated dropwise over 5 min with oxalyl chloride (0.37 mL, 4.2 mmol) under an N_2 atmosphere. The cooling bath was removed and the reaction mixture was allowed to slowly warm to room temperature and stirred there for 4 h. The reaction was evaporated to dryness in vacuo and dried under high vacuum (1 mm Hg) for 18 h to yield 260 mg (87%) as a yellow solid, which was carried on without further purification. ^{1}H NMR ($CDCl_3$, 500 MHz): δ 7.96 (s, 1H), 7.53 (d, J = 7.3 Hz, 2H), 7.40 (t, J = 7.3 Hz, 2H), 7.32 (t, J = 7.3 Hz, 1H), 7.22 (s, 1H), 2.05 (s, 3H), 1.96 (s, 3H).

*4.8. Synthesis of bis(DTE) **4***

A solution of bis(amidine) **1** (0.04 g, 0.14 mmol) and Et_3N (43 μL) in anhydrous CH_2Cl_2 (25 mL) was treated dropwise over 5 min with a solution of the carboxylic acid chloride of DTE **3** (157 mg, 0.31 mmol) in anhydrous CH_2Cl_2 (2 mL) at 0 °C under an N_2 atmosphere. After stirring for 30 min, the cooling bath was removed and the reaction was allowed to slowly warm to room temperature and stirred there for 5 h. The solvent was evaporated to a slurry, which was loaded to a short silica column (25 g silica, 4 cm high, CH_2Cl_2, 2.5% CH_3OH, 1% Et_3N). The resulting green solution was collected and evaporated to dryness. Purification by recrystallization (CH_3OH and CH_2Cl_2) yielded 122 mg (71%) of **4** as a green solid. mp = 176–177 °C. ^{1}H NMR ($CDCl_3$, 500 MHz): δ 12.95 (br s, 1H) 7.74 (s, 2H), 7.49 (d, J = 7.8 Hz, 4H), 7.36 (t, J = 7.8 Hz, 4H,), 7.28 (t, J = 7.8 Hz, 2H), 7.23 (s, 2H), 5.36 (s, 1H), 1.96 (s, 6H), 1.82 (s, 6H), 1.17 (s, 12H), 1.15 (s, 12H). ^{13}C NMR ($CDCl_3$, 100 MHz): δ 182.2, 177.1, 172.6, 149.2, 142.5, 141.7, 139.3, 133.4, 132.8, 129.1, 128.1, 125.7, 122.3, 90.40, 49.4, 47.9, 23.6, 22.8, 15.2, 14.6 (20 of 27 carbons found). FT-IR (KBr cast): 3435, 2978, 1685, 1654, 1624, 1590, 1542, 1499, 1458, 1380, 1338, 1276, 1191, 1137, 1107, 1058, 985, 756 cm^{-1}. MALDI m/z = 1228 [M + H]$^+$. Anal. Calcd for $C_{61}H_{52}N_4O_2S_4F_{12}$: C, 59.60; H, 4.26; N, 4.56. Found: C, 59.90; H, 4.26; N, 4.66.

*4.9. Synthesis of the bis(DTE) coordination compound **Zn4a***

A solution of bis(DTE) **4** (50 mg, 0.04 mmol) and Et_3N (6 μL, 0.04 mmol) in anhydrous CH_2Cl_2 (25 mL) was treated with a solution of the anhydrous $ZnCl_2$ (44 mg, 0.32 mmol) in anhydrous CH_3CN (25 mL) under an N_2 atmosphere. The solution was stirred for 5 h, at which time it was evaporated to dryness in vacuo and under high vacuum for 10 min. The solid residue was dissolved in CH_2Cl_2, the cloudy suspension was centrifuged and clear green solution was collected and evaporated to dryness. Purification by recrystallization two times (EtOAc) yielded 31 mg (57%) of **Zn4a** as a fine green powder. mp247–248 °C. ^{1}H NMR ($CDCl_3$, 400 MHz): δ 8.19 (s, 2H), 7.55 (d, J = 7.3 Hz, 4H), 7.39 (t, J = 7.3 Hz, 4H), 7.32–7.28 (m, 4H), 5.66 (s, 1H), 2.00 (s, 6H), 1.95 (s, 6H), 1.28 (s, 6H), 1.25 (s, 6H), 1.19 (s, 6H), 1.17 (s, 6H). ^{13}C NMR ($CDCl_3$, 125 MHz): δ 196.1, 191.3, 174.2, 151.8, 142.7, 141.7, 140.2, 135.2, 133.4, 129.1, 128.1, 127.0, 125.7, 122.2, 93.60, 51.0, 50.7, 25.0, 23.4, 22.7, 15.5, 15.4, 15.0, 14.9 (24 of 36 carbons found). FT-IR (KBr cast): 3433, 2980, 1599, 1561, 1499, 1451, 1365, 1336, 1270, 1231, 1192, 1105, 1056, 1031, 988, 893, 751 cm^{-1}. MALDI m/z = 1327 [M + H]$^+$. Anal. Calcd for $C_{61}H_{52}N_4O_2S_4F_{12}$: C, 55.12; H, 3.87; N, 4.22. Found: C, 54.80; H, 4.05; N, 3.95.

4.10. Photochemistry

The ring-closing reactions were carried out using the light source from a lamp used for visualizing TLC plates at 365 nm (Spectroline E-series, 470 W/cm^2). The ring-opening reactions were carried out using the light of a 150 W tungsten source passed through a 525 nm cutoff filter to eliminate higher energy light.

*4.11. Photochemical synthesis of the ring-closed isomer of bis(DTE) coordination compound (**Zn4b**)*

A solution of the ring-open isomer **Zn4a** (1.7 mg) in CD_2Cl_2 (0.55 mL) was irradiated in an NMR tube with 365 nm light using a hand held TLC lamp. The progress of the ring-closing reaction was monitored by ^{1}H NMR spectroscopy until a photostationary state was reached (after 30 min), yielding a solution containing 99% of **Zn4c**. The remaining 1% was assigned to the ring-open isomer **Zn4a**. ^{1}H NMR (CD_2Cl_2, 500 MHz): δ 8.16 (s, 1H), 7.62 (d, J = 7.8 Hz, 2H), 7.56 (d, J = 7.8 Hz, 2H), 7.48–7.43 (m, 3H), 7.39 (t, J = 7.8 Hz, 2H), 7.32–7.29 (m, 3H), 6.74 (s, 1H), 5.76 (s, 1H), 2.30 (s, 1.5H), 2.28 (s, 1.5H), 2.26 (s, 1.5 H), 2.24 (s, 1.5H), 2.05 (s, 3H), 1.99 (s, 3H), 1.29 (s, 6H), 1.23 (s, 6H), 1.21–1.18 (m, 12H).

4.12. Fluorescence quantum yield measurements

The fluorescence quantum yield was calculated using the following relationship

$$\Phi_{\mathrm{Zn4}} = \frac{\Phi_{\mathrm{s}} A_{\mathrm{s}} F_{\mathrm{Zn4}} \eta_{\mathrm{Zn4}}^2}{A_{\mathrm{Zn4}} F_{\mathrm{s}} \eta_{\mathrm{s}}^2}$$

where Φ, A and F are fluorescence quantum yields, the absorbances at the excitation wavelengths and the area of the emission spectra of the standard (s) and the photoresponsive hybrid compound (**Zn4**), respectively, and η is the refractive index of the solvents used for the measurements. Quinine bisulfate in 0.5 M H_2SO_4 was used as a primary standard (0.55) [39]. Solutions were prepared and diluted to give a matched absorbance ($\pm$0.005 absorbance units) of approximately 0.1 at the excitation wavelength (320 nm). Solutions were purged with N_2 for at least 20 min prior to measurement. Solutions were diluted to a lower concentration of fluorophore with deaerated solvent to obtain two data points for each measurement. Exposure times were kept to a minimum and resulted in a maximum 10% decrease in absorbance throughout the entire experiment resulting in, at most, 10% error in the calculated quantum yield values, which is within the error determined for the value.

4.13. Fluorescence lifetime measurements

Time-resolved fluorescence measurements were performed using an Edinburgh Instruments OB 920 single-photon counting system with a hydrogen flash lamp excitation source. The excitation and emission wavelengths were set to 470 and 502 nm, respectively, and the band pass for the excitation and emission monochromators was ca. 16 nm. An iris was employed to ensure that the frequency of the stop pulses was smaller than 2% of the start pulse frequency. The number of counts in the channel of maximum intensity was 2000. The instrument response function was collected using Ludox (Aldrich) to scatter light at the excitation wavelength. A Lauda RM6 bath was used to keep the sample at a constant temperature of 20 °C. Data were analyzed using the Edinburgh software. The instrument response function was deconvoluted from the experimental data, and the data were fitted to monoexponential decays. The value of χ^2 (0.9–1.1), and visual inspection of the residuals and the autocorrelation were used to determine the quality of the fit. Solutions were prepared by dissolving the compound in CH_2Cl_2 and diluting them such that the absorbance at the excitation wavelength (470 nm) was approximately 0.1. Solutions were purged with nitrogen for at least 20 min prior to measurement.

4.14. Preparation and characterization of thin films of ***Zn4a***

Quartz substrates (2.5 cm × 1.2 cm) were cleaned by sequentially rinsing them with acetone, EtOH and MeOH, and drying them with clean air immediately before spin-casting. Appropriate amounts of **Zn4a** and PMMA (120 000) were dissolved in $CHCl_3$ and filtered through 0.2 μm PTEF filters (S&S Biopath). The quartz substrates were saturated by dropwise adding the **Zn4a**/PMMA solutions to them using a syringe. Thin films were prepared by spin-casting using a Laurell WS-400A-6NPP/Lite spin-coater operating at 3000–6000 rpm. The thickness of each film was determined by spectroscopic ellipsometry using a Jovin-Yvon UVISEL spectroscopic ellipsometer. Both Δ and ψ were measured as a function of wavelength and fit to an amorphous model using the ellipsometry software provided by the company. The experimental data set and the calculated values were compared using an iterative fitting algorithm and calculated "the goodness fit parameter χ^2".

4.15. Electrochemistry

Cyclic voltammetry was performed using a Pine AFCBP1 bipotentiostat with a cell consisting of polished glassy carbon working electrode (3 mm diameter, bioanalytical systems) and 0.1 M Bu_4NPF_6 as the electrolyte. A platinum counter electrode and a silver wire reference electrode were used for **3a** and **3b** with CH_2Cl_2 as the solvent. A platinum counter electrode and a platinum reference electrode containing 0.1 M tetrabutylammonium iodide and 0.05 M I_2 in CH_3CN as the inner solution were used for **Zn5** with CH_3CN as the solvent. The CVs were acquired using 100 mV s^{-1} (for **Zn5**) and 300 mV s^{-1} (for **3a** and **3b**) scan rates.

4.16. Free energy of PET calculations

The free energies of photoinduced electron transfer were calculated using the Rehm equation [40]

$$\Delta G_{\mathrm{PET}} = 23.06 \left[E^0 \left(\frac{\mathrm{D}^+}{\mathrm{D}} \right) - E^0 \left(\frac{\mathrm{A}}{\mathrm{A}^-} \right) \right] - w_{\mathrm{p}} - \Delta G_{00}$$

where $E^0(\mathrm{D}^+/\mathrm{D})$ is the oxidation potential of **3a** (+1.806 V versus NHE) and **3b** (+0.939 V versus NHE), and $E^0(\mathrm{A}/\mathrm{A}^-)$ is the reduction potential of **Zn5** (−0.945 V versus NHE), w_{p} is the attractive Coulombic force between D^+ and A^- estimated using the following equation

$$w_{\mathrm{p}} = 332 \frac{(z_{\mathrm{D}^+})(z_{\mathrm{A}^-})}{d_{\mathrm{cc}} \varepsilon_{\mathrm{s}}}$$

$$w_{\mathrm{p}}(\boldsymbol{Zn5} \cdot \boldsymbol{3a}) = -3.49\,\mathrm{kcal\,mol^{-1}}$$

$$w_{\mathrm{p}}(\boldsymbol{Zn5} \cdot \boldsymbol{3a}) = -3.39\,\mathrm{kcal\,mol^{-1}}$$

where z_{D^+} and z_{A^-} are the charges on the molecules, d_{cc} is the center-to-center separations distance in Å between the two ions (10.5 Å and 10.8 Å for **Zn5**·**3a** and **Zn5**·**3b**, respectively) approximated using molecular models created with SpartanTM'02 for Macintosh, [41] and ε_{s} is the static dielectric constant of the solvent (9.08 for CH_2Cl_2).

ΔG_{00} is the change in free energy (60.2 kcal mol^{-1}) of the electron donor upon excitation with light calculated using

$$\Delta G_{00} = \frac{hcN_{\mathrm{A}}}{\lambda_{\mathrm{ex}}}$$

$$\Delta G\ \mathrm{PET}\ [\boldsymbol{Zn5} \cdot \boldsymbol{3a}] = 6.73\,\mathrm{kcal\,mol^{-1}}$$

$$\Delta G\ \mathrm{PET}\ [\boldsymbol{Zn5} \cdot \boldsymbol{3b}] = -13.36\,\mathrm{kcal\,mol^{-1}}$$

Acknowledgements

This work was supported by the Natural Sciences and Engineering Research Council of Canada, the Canada Research Chairs Program, Simon Fraser University and the University of Victoria. We are grateful to Nippon Zeon Corporation for supplying the octafluorocyclopentene needed to prepare the photochromic compounds and to Dr. C. Weymuth (University of Zurich) for kindly providing bis(amidine) **1**.

References

[1] B.L. Feringa (Ed.), Molecular Switches, Wiley-VCH, Weinheim, Germany, 2001.

[2] M. Irie, Chem. Rev. 100 (2000) 1685–1716.

[3] T.B. Norsten, N.R. Branda, J. Am. Chem. Soc. 123 (2001) 1784–1785.

[4] T.B. Norsten, N.R. Branda, Adv. Mater. 13 (2001) 347–349.

[5] A.J. Myles, N.R. Branda, J. Am. Chem. Soc. 123 (2001) 177–178.

[6] A.J. Myles, N.R. Branda, Adv. Funct. Mater. 12 (2002) 167–173.

[7] M.G. Tsivgoulis, J.-M. Lehn, Angew. Chem. Int. Ed. Engl. 34 (1995) 1119–1122.

[8] J.J.D. de, W.R. Browne, M. Walko, L.N. Lucas, L.J. Barrett, J.J. McGarvey, J.H.V. Esch, B.L. Feringa, Org. Biomol. Chem. (2006) 2387–2392.

[9] G. Jiang, S. Wang, W. Yuan, L. Jiang, Y. Song, H. Tian, D. Zhu, Chem. Matt. 18 (2006) 235–237.

[10] S.-J. Lim, B.-K. An, S.D. Jung, M.-A. Chung, S.Y. Park, Angew. Chem., Int. Ed. 43 (2004) 6346–6350.

[11] M.-Q. Zhu, L. Zhu, J.J. Han, W. Wu, J.K. Hurst, A.D.Q. Li, J. Am. Chem. Soc. 128 (2006) 4303–4309.

[12] M. Bossi, V. Belov, S. Polyakova, S.W. Hell, Angew. Chem. Int. Ed. 45 (2006) 7462–7465.

[13] F.M. Raymo, M. Tomasulo, J. Phys. Chem. 109 (2005) 7343–7352.

[14] K. Yagi, C.F. Soong, M. Irie, J. Org. Chem. 66 (2001) 5419–5423.

[15] J. Ern, A.T. Bens, H.-D. Martin, S. Mukamel, S. Tretiak, K. Tsyganenko, K. Kuldova, H.P. Trommsdorff, C. Kryschi, J. Phys. Chem. A 105 (2001) 1741–1749.

[16] H. Cho, E. Kim, Macromolecules 35 (2002) 8684–8687.

[17] M. Irie, T. Fukaminato, T. Sasaki, N. Tamai, T. Kawai, Nature 420 (2002) 759–760.

[18] M.-S. Kim, T. Kawai, M. Irie, Opt. Mater. 21 (2002) 271–274.

[19] J. Finden, T.K. Kunz, N.R. Branda, M.O. Wolf, Adv. Mater. 20 (2008) 1998–2002.

[20] T. Kawai, T. Sasaki, M. Irie, Chem. Commun. (2001) 711–712.

[21] G.M. Tsivgoulis, J.-M. Lehn, Chem. Eur. J. 2 (1996) 1399–1406.

[22] T.A. Golovkova, D.V. Kozlov, D.C. Neckers, J. Org. Chem. 70 (2005) 5545–5549.

[23] H. Tian, B. Chen, H. Tu, K. Müllen, Adv. Mater. 14 (2002) 918–923.

[24] R. Harter, C. Weymuth, R. Scheffold, Helv. Chim. Acta 76 (1993) 353–371.

[25] Following the procedures described in the thesis of Dr. C. Weymuth (University of Zurich).

[26] A.J. Myles, N.R. Branda, Macromolecules 36 (2003) 298–303.

[27] More detailed thermal stability studies using UV–vis absorption and ^{1}H NMR spectroscopy were carried out for **Zn4a** and control **Zn6** by comparing the changes in the spectra for solutions using 100% CH_2Cl_2, 50:50 CH_2Cl_2:CH_3CN and 100% CH_3CN. The UV–vis absorption spectrum of **Zn4a** showed no observable changes for the 100% CH_2Cl_2 solution but systematically changed until a completely new spectrum appeared within 3 h for the 100% CH_3CN solution and within 48 h for the CH_2Cl_2:CH_3CN solution. Compound **Zn5** showed the same phenomenon except that the spectral changes were significantly slower. Similar trends were observed for the ^{1}H NMR spectra.

[28] The lowest energy absorption band in the UV–vis spectrum for free ligand **6** appears at 373 nm.

[29] The ring-closing reactions were carried out using the light source from a lamp used for visualizing TLC plates at 365 nm (Spectroline E-series, 470 W/cm^2).

[30] The photostationary state was reached within the first minute of irradiation at the concentrations used for the UV–vis spectroscopy studies (1.3×10^{-5} M). The more concentrated solutions used for ^{1}H NMR spectroscopy (2.3×10^{-3} M in CD_2Cl_2) required longer irradiation times (typically 210 s).

[31] A. Peters, R. McDonald, N.R. Branda, Adv. Mater. Opt. Electron. 10 (2000) 245–249.

[32] The ring-opening reactions were carried out using the light of a 150 W tungsten source passed through a 525 nm cutoff filter to eliminate higher energy light.

[33] The measurements were carried out using 320 nm as the excitation light for two, reasons. (1) There was no reliable primary standard conveniently available for quantum yield determination that could be excited at, 470 nm. (2) Since 470 nm is very close to the edge of the emission spectrum, excitation at 470 nm doesn't allow for collection and integration of the entire fluorescence emission spectrum, which is necessary for accurate determination of the quantum, yield. Hybrid compound **Zn4a** undergoes photoinduced cyclization during the determination of the quantum yield if 470 nm was used resulting in calculated values lower than the true, ones.

[34] F.M. Raymo, M. Tomasulo, J. Phys. Chem. A 109 (2005) 7343–7352.

[35] T. Yamaguchi, M. Irie, J. Mater. Chem. 16 (2006) 4690–4694;
N. Xie, Y.J. Chen, J. Mater. Chem. 17 (2007) 861–865.

[36] N. Xie, Y. Chen, J. Mater. Chem. 17 (2007) 861–865.

[37] H.D. Samachetty, N.R. Branda, Pure Appl. Chem. 78 (2006) 2351–2359;
H. Samachetty, N.R. Branda, Chem. Commun. (2005) 2840–2842.

[38] Unfortunately due to difficulties encountered during recrystallization, the cobalt complex has yet to be isolated.

[39] S.L. Murov, I. Carmichael, L.H. Gordon, Handbook of Photochemistry, 2nd ed., Marcel Dekker, Inc., New York, 1993.

[40] G.J. Kavarnos, Fundamentals of Photoinduced Electron Transfer, VCH Publishers, Inc., New York, 1993.

[41] Spartan'02 for Macintosh, Wavefunction, Inc., Irvine.